**Proceedings of: ME2000**
**The 2000 International Mechanical Engineering Congress & Exposition**
**November 5-10, 2000, Orlando, Florida**

# HIGH-SPEED PASSENGER AND INTERCITY TRAIN AERODYNAMIC COMPUTER MODELING

Samuel Holmes
Applied Research Associates, Inc.
830 E. Evelyn Ave. Suite C
Sunnyvale, CA 94086

Martin Schroeder
Transportation Technology Center, Inc.
55500 D.O.T. Road
Pueblo, Colorado 81001

Elton Toma
Transportation Technology Center, Inc.
55500 D.O.T. Road
Pueblo, Colorado 81001

## ABSTRACT

With the onset of high-speed passenger train service in the United States, the Federal Railroad Administration (FRA) and railroad agencies are concerned with the aerodynamic effects these trains will have on lightweight freight equipment, such as empty double stack container cars. This paper presents the results of a research project that evaluated this interaction. In this study we conducted a series of computational fluid dynamic (CDF) calculations to characterize the aerodynamic loads on a container consist passed by a high-speed train. A train motion simulation program was used to determine resultant motion and risk of overturning or derailment of the container consist. Numerous cases were studied in which train speed and wind speed and direction were varied.

## INTRODUCTION

The purpose of this study is to examine the aerodynamic effects of the Acela high-speed passenger train on other trains in the Northeast Corridor. Several scenarios are examined here with the objective of assuring the safety of both Acela and other trains operating on adjacent tracks. This report examines the likelihood of container consist derailment due to the aerodynamic loads generated by the passing Acela.

This study focuses on establishing the possibility, but not the probability, of occurrence. Thus we have taken a worst case approach where possible in establishing the aerodynamic loads and the subsequent train response. Our approach to the passing trains problem is based on the use of Acusolve™ and NUCARS™ computer codes. Acusolve™ is a finite element code for the solution of incompressible viscous flow problems. NUCARS is a train motion simulation program that is used to determine the resultant motion and risk of derailment of the passing trains.

In order to facilitate the computational process, we separated the aerodynamic calculations from the dynamic response calculations. The implied assumption is that the small response motions of the container train will not influence the aerodynamic loads. A matrix of aerodynamic calculations was used to characterize the loads on the passing trains in terms of peak force and moment resultants as well as load duration and total impulse.

## BACKGROUND

Acela will pass many trains in the Northeast Corridor. We chose a double-stack container car in a 5-pack articulated consist with shared trucks for this study because this consist is characterized by a large surface area and a propensity for dynamic interaction between the cars which share trucks.

The container cars studied here utilize shared trucks between cars and are combined in an articulated string of five cars as shown in Figure 1. Each container car has an effective length (truck-to-truck center distance) of 58 feet 10 inches (18.7 m). Containers are stacked two high on the car. The lower containers sit in the well of the container car. This type of

container arrangement sometimes results in a staggered end on the container stack. The stack has a total height above track level of about 16 feet (4.9 m) and presents a large lateral surface area to Acela so that small changes in lateral pressure give rise to large lateral forces.

Figure 1. Generic double stack container car with containers

## TRAIN AERODYNAMICS

The aerodynamic loads on the container train were calculated using the Acusolve™ finite element computational fluid dynamics (CFD) solver. Acusolve™ uses unstructured grids enabling easier mesh generation. Two meshes representing a course and fine discretization were generated to model the contours of Acela and a container train on an adjacent track. The course mesh contains 92,682 hexahedral elements and 99,834 nodes and the fine mesh contains 305,868 hexahedral elements and 321,609 nodes. Figure 2. shows the overall mesh shape. The mesh, representing the fluid around Acela and the container train, is a parallelopiped with dimensions of 70 m long by 35 m wide by 20 m high. Figure 2 shows the surface of Acela (near train) and the surface of a container consist with a single container. The origin for the mesh is located at the front of Acela at the track level and Acela is facing in the positive X-direction. The container train is to the left of Acela.

In the CFD solution, the fluid mesh is fixed to the front of Acela so that all velocity boundary are specified relative to the Acela velocity. Also, the container consist is modeled as smooth with no breaks between the cars. The motion of the container(s) relative to Acela is modeled as a moving boundary condition, i.e. as a boundary condition on the nodes in the area above the container car. In this approach, the effect of the container is moved through the mesh while the mesh remains fixed [1]. As nodes enter the container volume, the boundary condition is applied so that the fluid velocity within the container is constrained to be the container velocity. Thus the momentum of the fluid within the moving boundary is constant and the pressure distribution on the boundary surface is the same as would occur if the boundary condition (i.e. the container velocity) were applied to the nodes defining the container surface.

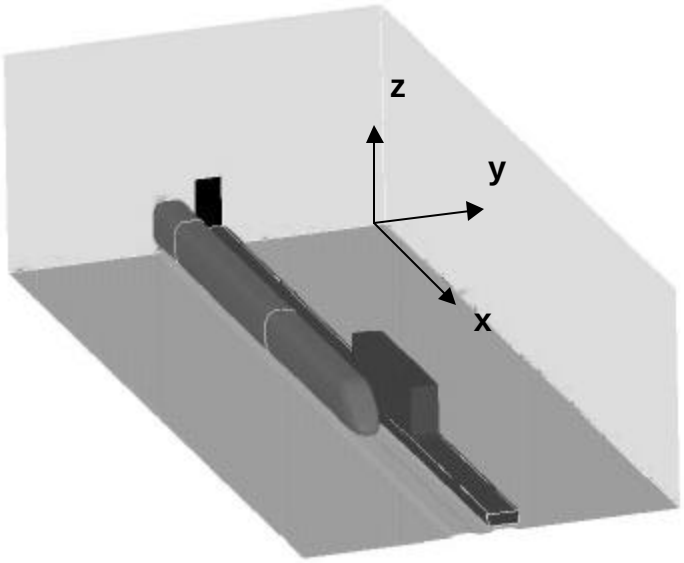


Figure 2. Mesh surfaces.

Figure 3 shows the coarse surface mesh of a container car and Acela as they pass near one another. Pressure contours are plotted on the mesh so that the dark areas are low pressure areas. Note that the mesh is refined near the nose of Acela and is considerably coarsened elsewhere. The container contours shown are for a container stack with staggered ends. We also modeled containers with simple straight ends as shown in Figure 2. By comparing the aerodynamic loads predicted for the two configurations we found that the simple configuration of gives slightly higher loads on the container car than the staggered configuration so we used the simple geometry for most of this study.

We believe that the primary variables affecting the aerodynamic loads are the velocities of Acela and the container train and the ambient wind speed and direction. Secondary variables are small changes in container geometry and the arrangement of the containers, that is, whether or not several container cars carry containers in a row vs. a single container surrounded by empty cars as shown in Figure 2.

A matrix of aerodynamic calculations was planned to cover a range of operation and ambient conditions and also to explore potential worst cases both from the point of view of aerodynamic interactions and from the point of view of container consist response. A total of 15 calculations were

completed in which we calculated the overall forces on a container consist. These are listed in Table 1 as Cases 1-15.

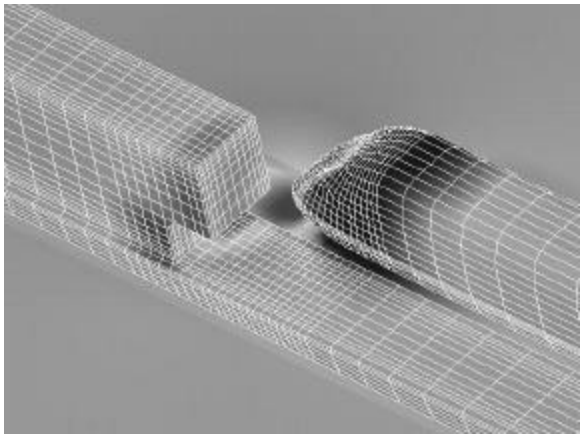

Figure 3. Staggered-end container simulated with moving boundary condition and Acela (coarse mesh).

Table 1. Analysis Matrix

| Case | Config.* | Train Velocity | | Wind | |
|---|---|---|---|---|---|
| | | Acela (mph) | Freight (mph) | X (mph) | Y (mph) |
| 1 | F-S-1 | 150 | -50 | 0 | 0 |
| 2 | F-S-3 | 150 | -50 | 0 | 0 |
| 3 | R-S-1 | 150 | -50 | 0 | 0 |
| 4 | F-C-1 | 150 | -50 | 0 | 0 |
| 5 | F-S-3 | 150 | -50 | -50 | 0 |
| 6 | F-S-1 | 150 | -50 | 50 | 0 |
| 7 | F-S-1 | 150 | 50 | 50 | 0 |
| 8 | F-S-1 | 150 | 50 | -50 | 0 |
| 9 | F-S-1 | 150 | -50 | 0 | -50 |
| 10 | F-S-1 | 150 | 30 | 50 | 0 |
| 11 | F-S-1 | 150 | 15 | 50 | 0 |
| 12 | F-S-1 | 150 | 30 | -50 | 0 |
| 13 | F-S-1 | 150 | 15 | -50 | 0 |
| 14 | R-S-1 | 150 | 50 | -50 | -50 |
| 15 | F-S-1 | 120 | 50 | -50 | 0 |

*Gives interaction location (F = front, R = rear) container end geometry (S = simple, C = staggered) and number of containers in row.

The analysis of Acela meeting a container train moving in the opposite direction is used here to illustrate the basic features of the interaction problem and the data reduction procedure. In this first case, Acela is moving at a velocity of 150 mph (67.0 m/s) towards a container train moving in the opposite direction at 50 mph (22.35 m/s) in still air. With a closing speed of 200 mph (89.4 m/s) the 18.7 m long container car passes a point on Acela in 0.21 seconds.

The solution for this example (Case 1) was obtained using the Acusolve™ finite element code. Acusolve™ solves the incompressible Navier Stokes equations and has provisions for turbulence modeling. However, in order to simplify our calculations and reduce mesh size (the number of nodes) we did not model turbulence or the boundary layer on the trains and our solutions are in effect Euler solutions of the flow. Thus we expect to resolve the pressure loads on the container consist and not the viscous contributions to the aerodynamic load. We believe that this is an acceptable approximation because the changing pressure distribution on the cars contributes most to the load for these blunt shapes [2].

In Case 1, we used the coarse mesh and 150 time steps of 0.005 seconds each. After completion, the solution was post-processed to examine the flow and to obtain pressure contours on the surface of Acela and the container train. In addition, the load history on the container car was derived by integrating the surface pressure over the car and container surfaces. This analysis showed an interaction pattern that is repeated for all of the cases for interaction at the head-end of Acela. However, the magnitude and duration of the load and some of the load features change with the problem parameters.

Figure 4 shows the pressure contours on the Acela locomotive and container car at an instant during the passing sequence. The load on the container car is determined principally by the pressure distribution around Acela. The features of this distribution are a high pressure region ahead of Acela (light contours) and a low pressure region on the sides of the Acela locomotive (dark contours). As these regions pass the container car they exert a push-pull lateral motion on the car as well as strong yaw moments. The force and moment resultants on the car are plotted in Figures 5 and 6. Note that the moments are taken about the car center at the track level. In these figures, the times t1 and t2 indicate the points at which the locomotive reaches the front and back of the container car.

Examining the force histories plotted in Figure 5, we see the lateral push pull effect in the Y-component of the force resultant. Changes in lift (Z-component) and drag (X-

component) are also seen but these components are not as large as the lateral component.

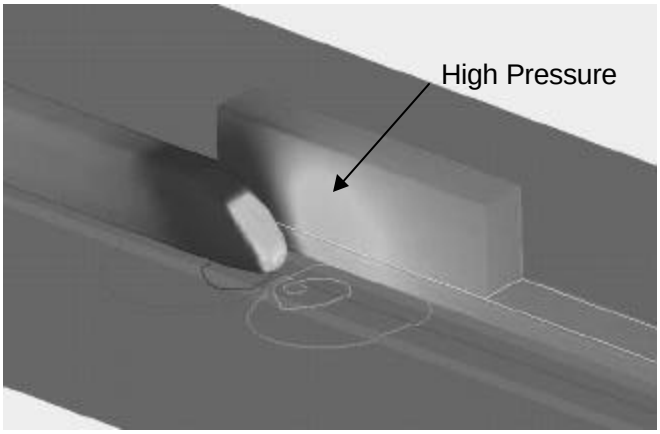


Figure 4. Pressure contours on Acela and container consist.

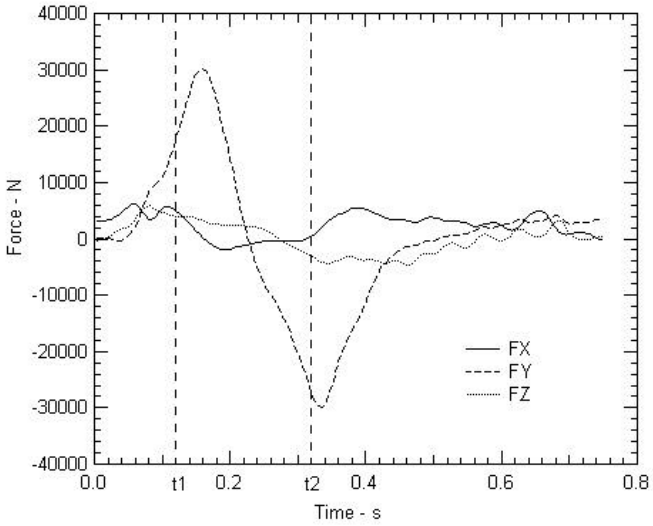


Figure 5. Force resultant histories for Case 1.

Figure 6 shows the moments on the container car during the passing sequence. Here the aerodynamic loads exert a strong rolling (MX) and yaw (MZ) moment on the car. These are out of phase because the strongest yaw moment occurs when the Acela locomotive is alongside the car and the high pressure ahead of Acela is pushing on the back end of the container while the low pressure on the side of Acela is pulling on the container. At this time the lateral force goes to zero. Figure 6 also shows a large pitching moment (MY) due to changes in airflow under the container consist. Although these moments are large, they have little effect on the consist because the car has a large resistance to pitching motions. Note also that some of these curves show an oscillation at late times. This is due to the effect of the moving boundary condition as it moves through coarse regions of the mesh. In general, these effects are small although we used smoothing techniques on some problems in order to make the data easier to interpret [1].

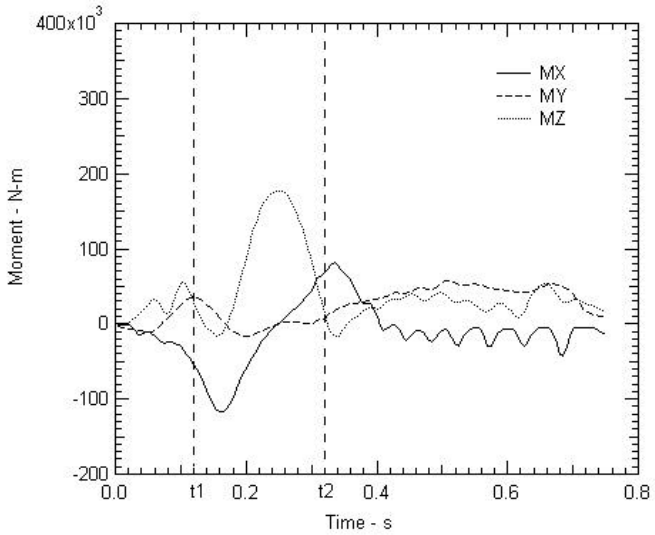


Figure 6. Moment resultant histories for Case 1.

The pattern of forces and moments on the container consist are similar for all of the simulations in Table 1 for interaction at the head-end of Acela. However, we found that the maximum lateral load amplitude occurs when Acela is at maximum velocity (150 mph) and faces a head wind[1]. The lateral loads were lowest when Acela has a tail wind. As might be expected, the introduction of a strong (50m mph) cross wind creates a large mean lateral load and rolling moment on the container consist. We also found that the timing and duration of the loads can be varied by changing the direction and speed of the two trains as they pass one-another. In effect, the load duration varies proportionally with the passing time. This latter effect is important because if the two trains are running in the same direction, the load duration increases substantially and the total impulse on the container cars increases. Also, the load characteristic time can be made to correspond to natural periods of container consist motion.

## CONTAINER CONSIST DYNAMIC RESPONSE

We believe that vehicles posing the highest risk for derailment or dynamic instability due to aerodynamic forces are those with large surface areas and lightly damped and coupled dynamical behavior. For freight applications, a double-stack container car in a 5-pack articulated configuration loaded with two levels of containers provides large surface area and the propensity for dynamic interaction between cars with shared trucks.

1 Wind speed was limited to 22.35 m/s (50 mph) in this study.

We used A the NUCARS analysis tool to assess the degree of safety risk associated with high-speed passes of Acela trains. The NUCARS computer model is a general-purpose code that simulates the time domain response of vehicle rigid-body/flexible-body dynamic modes, and reaction forces between wheels and rails. The model allows for a wide variation in specified load environments such as the inclusion of wind vectors, inter-body connections, gravity, and other forces or moments. NUCARS is also well adapted to simulate the nonlinear interaction forces produced at wheel and rail contact areas, and is recognized as one of the pre-eminent models that effectively treat these interactions. The particular car models used in this study had been previously verified against actual test data.

In each NUCARS simulation, the aerodynamic loads on the container train were taken directly from the CFD solutions. NUCARS was used to model container consist response for both loaded and empty consist. Some partially loaded consists were also analyzed.

A number of specific criteria are used to assess stability and safety including vertical wheel loading, the ratio of lateral to vertical wheel loads, wheel to rail contact angle, and general body motions of the car. Lateral to vertical wheel load ratios of 1.0, or higher, given a wheel angle of attack that is less than 5 milliradian, is the upper limit for safety according to Association of American Railroads (AAR) Chapter XI specifications (Manual of Standards and Recommended Practices, 1997). The degree of safety is assessed using these criteria. Wheel unloading and high lateral loads or large wheel to rail angle of attack can be precursors to increased safety risk or derailment and are therefore analyzed as part of the study. Additionally, whole body dynamic behavior quantified by predictions of roll, yaw, pitch and bounce amplitudes are used to evaluate car body envelope variations and general car-to-car dynamic displacements. Finally, the track model used for these analyses was established using measured data from actual track at the Transportation Technology Center (TTC) in Pueblo CO., which contains slight perturbations along the length of rails and across rails at levels normally expected for class-4 freight track.

Our studies show that both load amplitude and duration have a strong effect on consist response, especially when loading periods are near natural periods of response for the consist. In order to best explore how these factors affect consist stability, we planned our simulations around three loading scenarios that we thought might cause derailment. These are: 1) maximum aerodynamic resultant force and moment, 2) maximum lateral impulse and 3) “synchronized” load and response timing. Loads of the first type occur when both trains are traveling at high speed in opposite direction and when Acela faces a headwind. Load cases of the second type occur when both trains are traveling in the same direction at high speed. Loads of the third type occur when both trains are traveling in the same direction with Acela traveling at an intermediate speed so that the closing speed is reduced. In this later case, the load duration can be on the order of the period of vibration for some response modes of the container consist. As the load travels from car to car along the consist it appears to build the amplitude of these modes.

Most of the loading scenarios that were investigated used container cars loaded with empty containers as worst-case representations. Lightly loaded cars were found more likely to experience wheel unloading and large lateral-to-vertical wheel load ratios, which increase the risk of derailment. Two other cases were examined that included partially loaded and fully loaded containers, but in all cases the cars contained double-stack containers either empty or full as illustrated by the lead car of Figure 1.

The NUCARS analyses showed that Cases 8 and 9 and Cases 12 to 14 of Table 1 show the largest propensity for vehicle instability, and in fact for some cases showed wheel lift for time periods extending from 0.5 seconds to nearly 2.0 seconds and to near derailment conditions. Case 8 shows the largest impulse, while Cases 12 and 13 excite consist resonant modes. Cases 9 and 14 examine worst case loading caused by lateral wind vectors coupled with negative wind pulses generated at the end of the high-speed train. These last two cases produce serious consist motions. The largest peak aerodynamic load, noted in Case 5, produced less severe dynamic behavior, and although the peak load was large it was short in duration. Little dynamic response was therefore noted. Such high loads could be significant however, in the analyses of container attachment integrity or passenger window loads.

Similar analyses using partially loaded and fully loaded double-stack container cars showed improvement in dynamic stability. Fully loading all containers within the consist eliminated wheel lift and kept wheel L/V ratios much below 1.0, whereas consists with only the first and last cars loaded with all others empty, continued to show some signs of wheel lift, albeit minor and brief in duration. From examination of car body dynamic behavior, roll motion is slight for all cases considered and therefore, vehicle weight is the most important parameter affecting wheel unloading. Wheel unloading, which will be shown in later data plots is a result of lateral motion rather than car body roll so we expect that uneven container loading from top to bottom, which has an effect on roll inertia, has less influence than the overall weight of the car.

The largest lateral impulse was seen in Case 8 which we use an example here. In this example, the high-speed train operating at a speed of 150 mph (67 m/s) overtakes the freight consist traveling at 50 mph (22.35 m/s), resulting in a closing speed of 100 mph (44.65 m/s). The wind velocity is 50 mph opposing the high-speed train. For this worst case condition, the freight car roll and yaw motions between adjacent cars are generally out of phase, with some indication of amplification as

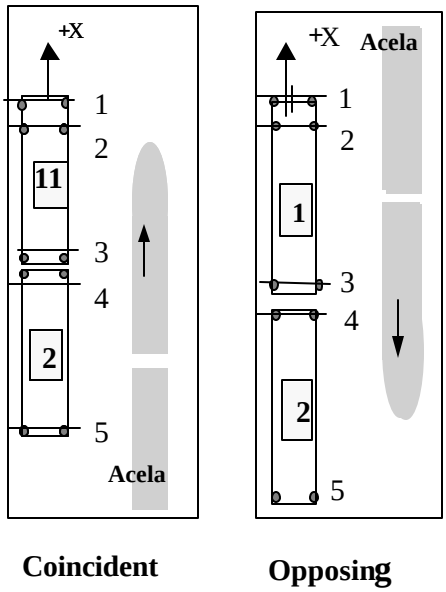


Figure 7. Schematic of trains with axle numbering system.

the high-speed train reaches the last car in the consist, noted as car number 1. Using the car and axle numbering system shown in Figure 7, Figures 8 and 9 show the roll and yaw motion of each freight car in the consist. Notice that Car 5 reacts first because the high-speed train initially overtakes from the rear of the freight train beginning at car 5 with Car 1 at the head of the freight consist. The largest roll motion is seen in car 1 and the largest yaw motion is seen in Car 5. We also found that cars 1 and 5 have the largest lateral displacements. Both the lead car (1) and trail car (5) can be expected to behave differently from the intermediate cars within the consist because these end cars do not share trucks on one of their ends and these trucks are therefore more lightly loaded. The ends of these cars can be expected to have larger dynamic motions and a greater risk for wheel unloading. All cases in this study showed that derailment is more likely to begin at the end cars.

Wheel loads for the first truck in the consist are plotted in Figure 10. Looking closer at wheel loads of Car 1, axle 1, we see that wheel loading becomes zero on the right wheel nearest the Acela, indicative of wheel lift initiated at the point of a maximum lateral wheel shift into flange contact. Note the load shifting between the left and right wheels 180 degrees out of phase indicating rocking. However, the lateral loads at flange contact however are modest with a maximum value of only ]9800 N (2200 pounds) indicating that there is insufficient force to initiate flange climb. Thus, derailment is unlikely.

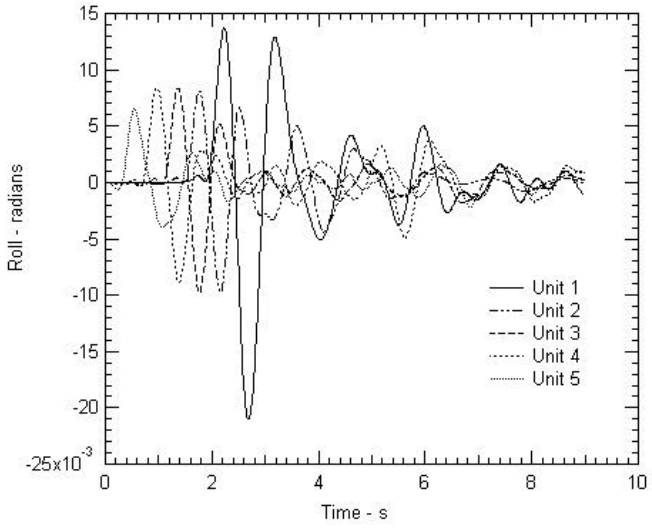


Figure 8. Roll motion of Container Cars, Case 8

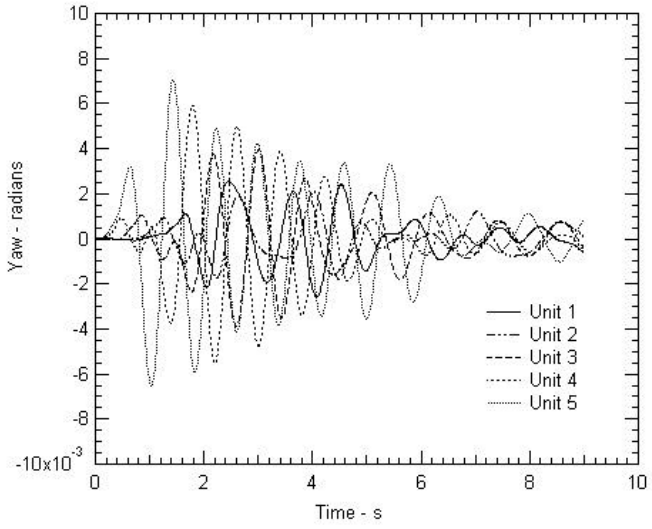


Figure 9. Yaw motion of container cars, Case 8

We found the worst cases in terms of potential derailment when the load duration was on the order of the consist natural periods of response. This is seen in Cases10, 11, 12, 13, 15, and to some degree, Case 8. Independent calculations with NUCARS predicted that lateral vibration modes have a temporal period of approximately 0.20 seconds, corresponding to a train closing speed of approximately 58 m/s (130 mph). NUCARS predictions showed that Case 12 at a closing speed of 54 m/s (120 mph) produces the highest magnitude and duration of wheel unloading.. Figure 11 plots the vertical force at Truck 1. Note the cyclic nature of wheel unloading, which continues after the Acela has passed (after 2.5 seconds). The cyclic nature of Car 1 is initiated when the Acela has just reached car-2, at a

time of approximately 1 second. Large amplitude fluctuations are seen when the Acela reaches the first car at a time of 1.7 seconds. The Acela is completely past the freight consist at a time greater than 2.5 seconds, after which the consist continues large amplitude cyclic wheel unloading behavior. Computation of these times is based on a consist length of approximately 107 m (350 feet), a car length of approximately 18 m (60 feet), and a closing speed of 54 m/s (120 mph).

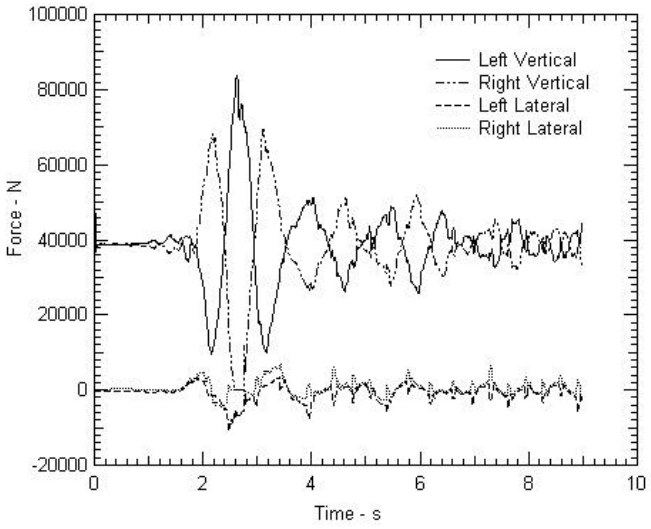


Figure 10. Lateral and vertical wheel loads, truck 1, axle 1, Case 8

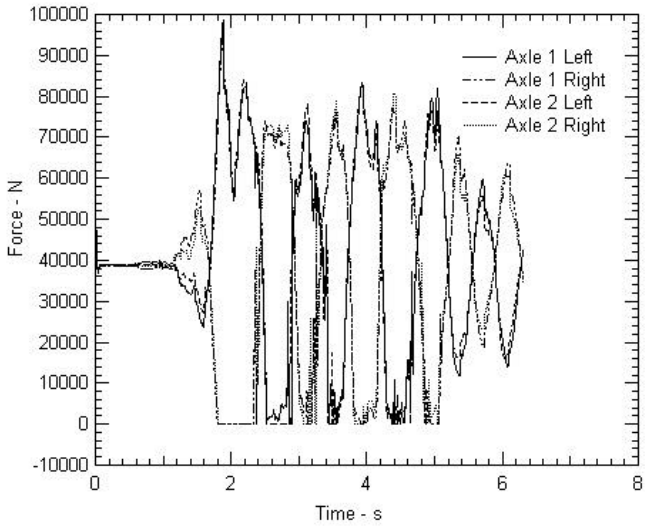


Figure 11. Vertical Force at Wheels of Container Car, Truck 1, Case 12

Figure 12 shows the vertical wheel loads of truck-2 (axles 3 and 4) of the first car. Note the difference between the second truck and the first truck shown in Figure 11. We believe that the reason truck-1 (axles 1 and 2) has more unloading is because the first truck is not shared, and therefore is lightly loaded. The first truck also has a standard coupler at its end, while the second truck is connected on both ends using articulated connections. For both trucks of Car 1, wheel lift exceeds AAR standards.

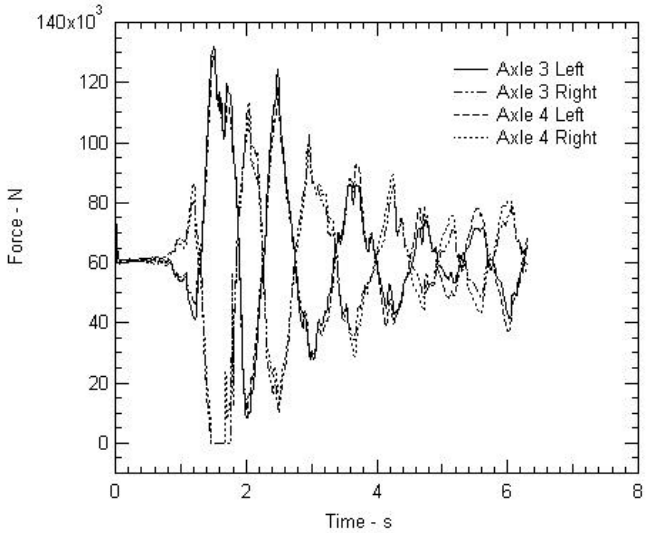


Figure 12. Vertical force at wheels of container car, truck 2, Case 12

## CONCLUSIONS

This study combined CFD simulation of the unsteady airflow over passing trains with a vehicle dynamic model to obtain container car response. The study focused on the Acela high speed train and a freight container consist with shared trucks. Our objective was to determine if derailment is possible rather than the likelihood of derailment. Consequently, we selected combinations of operating conditions and system configurations to examine worst-case scenarios. We found derailment unlikely under the many operating conditions, especially for fully loaded consists moving in opposite directions. However, we also found derailment likely under certain circumstances. Further studies may be warranted to more precisely determine safe operating conditions.

The CFD calculations showed that the aerodynamic loads are characterized by a load sequence that occurs primarily at the front end and the back end of Acela. The opposing cars are subjected to a lateral push-pull force causing both rolling and yawing moments. These loads seem to be the most significant in determining the motion of the container consist. We found that the amplitude of the load depends most on Acela speed and the presence of a headwind. The load timing depends on the closing velocity of the two trains. The presence of a crosswind can increase the absolute magnitude of the lateral load

significantly but does not increase the dynamic component of the load.

We found that the maximum aerodynamic forces on the container trains occur when it moves in the opposite direction to Acela and when Acela faces a headwind. The maximum impulse is generated when the two trains move in the same direction. Intermediate speeds producing long pulse durations tend to maximize response and the risk of derailment. These analyses show that under the most commonly encountered conditions of loaded container cars passing Acela in the opposite direction, the container consist response is benign. However, several specific combinations of train speed and direction and container and wind speed pose a high risk of derailment. This is lessened for fully loaded container trains traveling in the opposite direction with little or no wind.

## REFERENCES


1. Holmes, B. S., Dias, J., Rafai,S. M., J., Buell, J.C, Johan, Z., Sassa, T., and Sato, T., "Solution of train-tunnel entry flow using parallel computing," Computational Mechanics 23 (1999) 124-129
2. Anderson, J. D., "Fundamentals of Aerodynamics," McGraw Hill, New York (1991) pp. 54-61


## ACKNOWLEDGMENTS


This work was supported by the Federal Railroad Administration through the Volpe National Transportation Systems Center. The authors especially wish to thank James H. Lamond of the Volpe National Transportation Systems Center for his guidance and support during the course of this work.